Scanning Microscopy

Volume 2 | Number 3 Article 18

7-7-1988

The Influence of Analyser Geometry Effects in Scanning Electron Microscope Voltage Contrast Measurements

Daniel S.H. Chan
National University of Singapore

Teck Seng Low
National University of Singapore

Wai Kin Chim
National University of Singapore

Jacob C. H. Phang
National University of Singapore

Follow this and additional works at: https://digitalcommons.usu.edu/microscopy

Part of the Biology Commons

Recommended Citation

Chan, Daniel S.H.; Low, Teck Seng; Chim, Wai Kin; and Phang, Jacob C. H. (1988) "The Influence of Analyser Geometry Effects in Scanning Electron Microscope Voltage Contrast Measurements," *Scanning Microscopy*: Vol. 2 : No. 3 , Article 18.
Available at: https://digitalcommons.usu.edu/microscopy/vol2/iss3/18

This Article is brought to you for free and open access by the Western Dairy Center at DigitalCommons@USU. It has been accepted for inclusion in Scanning Microscopy by an authorized administrator of DigitalCommons@USU. For more information, please contact digitalcommons@usu.edu.

Scanning Microscopy, Vol. 2, No. 3, 1988 (Pages 1419-1426)
Scanning Microscopy International, Chicago (AMF O'Hare), IL 60666 USA
0891-7035/88$3.00+.00

THE INFLUENCE OF ANALYSER GEOMETRY EFFECTS IN SCANNING ELECTRON MICROSCOPE VOLTAGE CONTRAST MEASUREMENTS

Daniel SH Chan*, Teck Seng Low, Wai Kin Chim and Jacob CH Phang

Electrical Engineering Department
National University of Singapore
10 Kent Ridge Crescent
Singapore 0511
Republic of Singapore.

(Received for publication March 01, 1988, and in revised form July 07, 1988)

Abstract

A computer simulation model used to study specimen dependent and analyser geometry dependent effects is described in this paper. With this model, the influence of the specimen dependent effect on quantitative voltage contrast measurements can be isolated from the analyser geometry dependent effect. Linearization error voltages in quantitative voltage contrast measurements arising from the individual influences of the specimen dependent and analyser geometry dependent effects are presented. The results show that the error component due to very narrow analysers dominate the total linearization error. The same situation arises when the voltage measurement point on the specimen is very near to the edge of the analyser.

KEY WORDS: Voltage contrast, scanning electron microscope, secondary electrons, energy analyser geometry, local field effects, error voltages, potential calculations, electron trajectories, electron beam testing, integrated circuits.

Address for correspondence:

D.S.H. Chan, National University of Singapore, Department of Electrical Engineering, 10 Kent Ridge Crescent, Singapore 0511. (Phone No. 772-2117)

Introduction

The use of the scanning electron microscope (SEM) in the voltage contrast mode is fast replacing the conventional mechanical probe for failure analysis of integrated circuits (ICs) as it possesses higher spatial and temporal resolutions. The use of the SEM also causes less damage to the specimen than mechanical probing.

Many studies [6,9,10] have been carried out on the use of voltage contrast as a voltage measurement technique. The main problem limiting the accuracy of this technique is the presence of local fields which arise from the spatially varying potentials and the finite size of the specimen conductors. However most of these studies on quantitative voltage contrast have usually simulated and measured these effects using a particular combination of specimen and analyser design. The results obtained are therefore only applicable to that particular analyser-specimen configuration. A more general approach would be to view the voltage contrast inaccuracies as being due to a combination of two types of effects, namely specimen dependent and analyser geometry dependent effects [2]. The fundamental effect of the potential barrier set up by local fields on the emitted SEs is defined as the specimen dependent effect. The influence of the spatial dimension of the analyser grids affecting the collection of SEs which have sufficient energy to overcome the potential barrier is termed the analyser geometry dependent effect. The separation of local field errors into these two components enables a better understanding of the mechanisms limiting voltage contrast accuracy. This understanding can be used in the design of efficient and accurate analysers.

This paper describes a simulation model which can be used for studying specimen dependent and analyser geometry dependent effects on SEM voltage contrast. Using computer simulation techniques, we have isolated the specimen dependent effect from the analyser geometry dependent effect. Linearization error voltages in quantitative voltage contrast measurements arising from the individual influences of the specimen dependent and analyser geometry dependent effects are presented. The relationship between the extraction field and the analyser

geometry dependent effect is also shown.

Principle of Quantitative Voltage Contrast Measurements

The quantitative determination of surface potentials using voltage contrast is based on the measurement of the energy distribution of secondary electrons (SEs) emitted from the surface. If the voltage at a measurement point changes by δV_s, then the potential energy of the SE emitted will also change by e δV_s, thus causing a shift in the SE energy distribution. SE energy distributions can be measured using an energy analyser, an example of which is shown in Fig. 1(a). This analyser has three grids - the extraction, retarding and reflection grids whose voltages are denoted by V_{ex}, V_r and V_{re}, respectively.

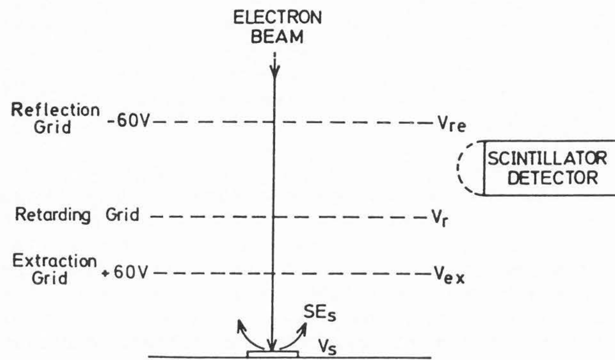

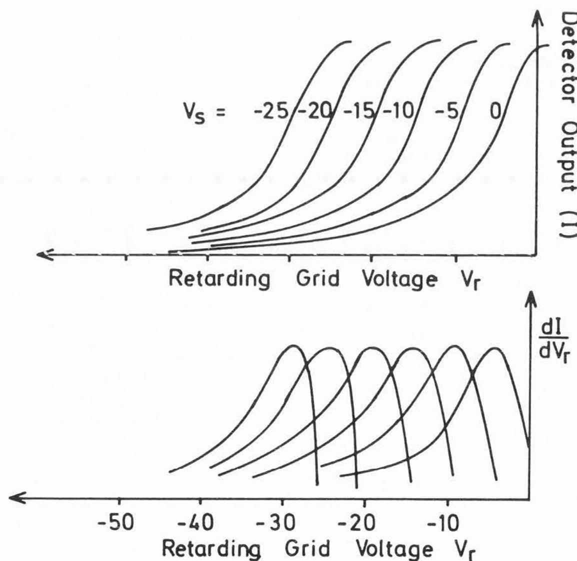

Fig. 1: (a) Schematic drawing of a retarding field energy analyser, (b) Output current of scintillator detector with varying voltage V_r, (c) Differential detector current showing shift in secondary electron energy.

If the voltage at the retarding grid is held at -2 V, then only SEs with energy greater than 2 eV will be able to cross the retarding grid to be collected by the detector. Thus the detector current will be an indication of the total number of emitted SEs with energy greater than 2 eV. Similarly, when V_r is set at -3 V, the detector current gives an indication of the total number of SEs with energy greater than 3 eV. The plot of the detector current as V_r is swept from 0 to -50 V producing an 'S-curve', and the differentiation of the S-curve gives the energy distribution of SEs emitted from the beam impact area. These can be seen in Figs. 1(b) and (c).

The shift in the SE energy distribution is commonly measured by the feedback approach in which the voltage at the retarding grid V_r is varied so as to keep the signal detected constant (Fig. 2). The change in the retarding grid voltage δV_r is equivalent to the shift in the SE energy distribution. In this approach, some feedback circuitry is employed to maintain a constant detector current. This method with variations has been used by different groups [3,4,5,10,12,13].

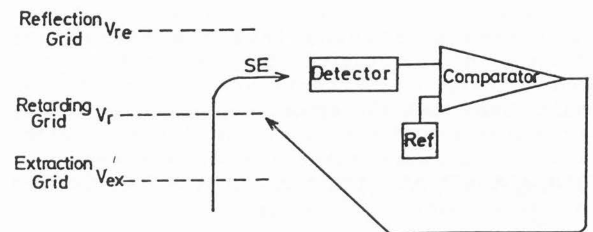

Fig. 2: A retarding field energy analyser with a feedback loop which maintains a constant detector current.

Although the shift in SE energy distribution is directly related to the surface potential at the emission area, accurate measurement of this shift becomes difficult under certain conditions. The inaccuracies are due to the existence of local fields near the specimen surface. [6,9].

If the specimen whose potential is to be measured consists of a conductor of finite width surrounded by other regions at different potentials, then a potential barrier will be created between the specimen and the extractor grid. This is illustrated in Fig. 3 where SEs emitted from the specimen have to cross a barrier of 4.22 V before being collected. This barrier filters out the low energy SEs, thus affecting the detector current and introducing non-linearities to potential measurement especially if the feedback method is used. The height of this barrier and the magnitude of the errors are dependent on the potential of the conductor and its physical dimensions. This phenomenon is known as type I local field effect and gives rise to linearization error, such that the shift in the retarding grid voltage is no longer equal to the change in the specimen voltage.

The potential of conductors in the general vicinity of the potential measurement point also affects the accuracy of the result. This is because these surrounding potentials exert a lateral force on the SEs and also affects the number of SEs collected. The effect of the surrounding potentials, known as type II local field effect, depends on the proximity of these potentials and their magnitude, but their effect can be seen in terms of their effect on the potential barrier. Type II local field effect will cause an error known as false voltage in quantitative voltage contrast measurements.

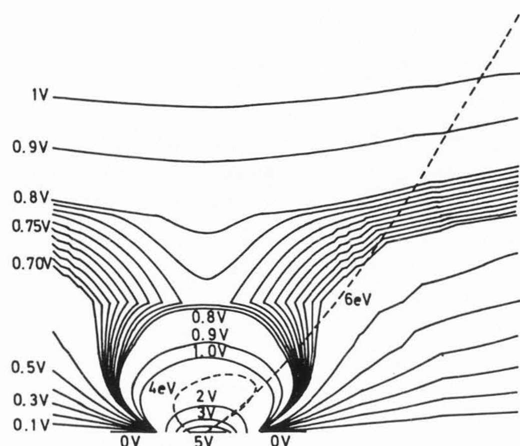

Fig. 3: Equipotential contours (solid lines) above a 3-electrode structure in a retarding field energy analyser with voltages (V_1,V_S,V_2) = (0,5,0) V and an extraction field of 10 V/mm. Trajectories of a 4 eV and a 6 eV electron (broken lines) are also shown to illustrate the effect of the 4.22 V potential barrier.

Before voltage contrast can be applied widely for quantifying surface potentials, the limitations on the accuracy of the method posed by the local field effects have to be reduced. There is, therefore, a need to obtain a better understanding of the different factors giving rise to error voltages in SEM voltage contrast. In particular, the effects of analyser geometry seem to have been neglected. Using a computer model, this effect is here isolated from the specimen dependent effect to give a better understanding of its contribution to error voltages.

A Simulation Model for Studying Specimen Dependent and Analyser Geometry Dependent Effects on SEM Voltage Contrast

Simulation Model

The model used for studying specimen dependent and analyser geometry dependent effects on SEM voltage contrast is shown in Fig. 4. The specimen consists of three electrodes - specimen electrode and two neighbouring electrodes whose voltages are denoted by V_S, V_1 and V_2, respectively. The electrode dimensions, a, and inter-electrode, b, spacing are both 5 μms. Type I local field effect can be studied by varying the specimen bias V_S and keeping both the neighbouring electrode voltages, V_1 and V_2, at zero; while type II local field effect can be studied by setting either V_1 or V_2 to a non-zero value.

In this model, we assume that the analyser grid meshes are fine enough for the extraction and retarding grids to be represented as equipotential surfaces. The width of the space being modelled was chosen to be 2 mm. The reason for this choice is to save on storage and computational requirements. This however does not affect the validity of the results as local fields exert an influence only around the vicinity of the electrodes which at most is in the lower region of tens of microns. Furthermore, the effect of the actual width of the extraction grid and its distance from the specimen plane on the SE trajectories can be taken into account by choosing the appropriate collection criterion y_c so that only those electrons which reach a certain height y_c above the specimen plane in Fig. 4 will be considered as being collected. The variation of parameter y_c has the same qualitative effect as varying the width of the extraction grid and the spacing between the extraction grid and the specimen plane of the practical energy analyser. The ideal case of a detector which is infinitely wide and very close to the specimen corresponds to a y_c value of near 0mm. In this case, all SEs that have left the potential barrier are regarded to have been collected.

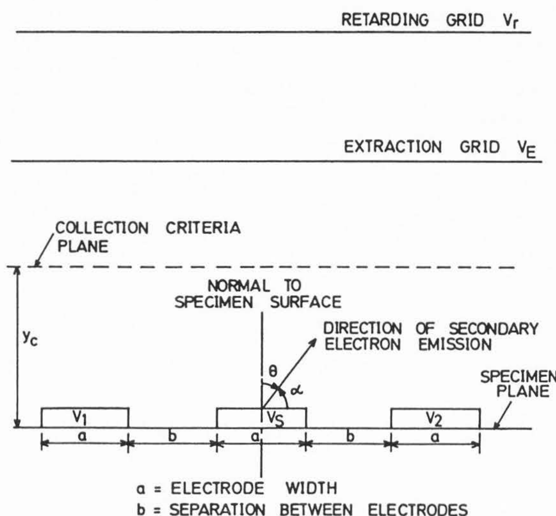

Fig. 4: Model of the planar retarding field energy analyser, with an extraction field, used in the theoretical study. (Dimensions: a = b = 5 μm)

Choice of Simulation Parameters

For the purposes of this study, values of y_c were set to be 0.5 mm, 1 mm and 2 mm.

Moderately weak extraction fields ranging from 10 V/mm to 100 V/mm were also chosen in this study. Although a weak extraction field may lead to larger error voltages in SEM voltage contrast measurements [6,9,10], weak fields are necessary in low accelerating beam voltage situations where a high extraction field will cause undesirable interference with the primary electron beam. There are several advantages associated with low accelerating beam voltage applications. The use of a low accelerating beam voltage means that only a small beam blanking voltage is required for stroboscopic voltage contrast imaging. Also the undesirable charging of passivated specimens can be avoided with low accelerating beam voltages. It has also been observed that high extraction voltages lead to a stretching of the S curves with a consequent loss of voltage resolution [8,11].

Method of Analysis

A finite element program is used to solve for the potential field distribution above the specimen surface, after which a trajectory tracking algorithm is used to compute the SE trajectories [1]. The advantages of using the finite element method over the more commonly used finite difference method and the description of the SE trajectory tracking algorithm used have been discussed [1]. From computing the SE trajectories, an acceptance diagram (Fig. 5) can be obtained. The SE collection angle in this figure is defined as the range of angles α of SE emission, measured from the horizontal in a counter-clockwise direction (Fig. 4) which are collected by the detector. The acceptance cone in Fig. 5 is the area which lies within the bounded lines and is shown as the shaded region in the figure. The lower energy limit of the acceptance cone corresponds to the potential barrier.

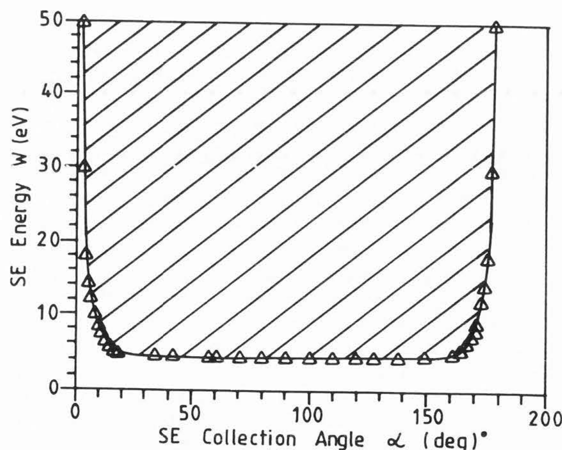

Fig. 5: Acceptance diagram for (V_1, V_s, V_2) = (0,5,0) V and a 10V/mm extraction field.

The energy distribution, N(W) of SE from metals was measured by Kollath [7] and his results were used in this study in the form of the following fitted equation:

$$N(W) = 1.5\, W \exp\,[2 - (8W/3)^{1/2}] \quad (1)$$

where W is the SE energy.

Using eqn. (1) and assuming Lambert's cosine law for the SE emission, the SE current collected by the detector for each SE energy W can be calculated as follows:

$$I(W) = N(W) \int_{\theta_{min}}^{\theta_{max}} \cos\theta \, d\theta \quad (2)$$

where θ_{min} and θ_{max} are the minimum and maximum acceptance angles for a particular SE energy W. The definition of θ is as shown in Fig. 4.

Changing the variable from θ to α (Fig. 4), where

$$\alpha = 90^{\circ} - \theta \quad (3)$$

equation (2) can be rewritten as follows:

$$I(W) = N(W)\, [\cos\alpha_{min} - \cos\alpha_{max}] \quad (4)$$

From eqn. (4), a curve of SE current versus SE energy can be plotted. S-curves, which are plots of total SE current versus retarding voltage V_r, and modified S-curves, the plots of total SE current versus $(V_s - V_r)$, can then be obtained from the curve of SE current versus SE energy by integrating the latter from a lower limit, equal to $(V_s - V_r)$, up to 50 eV, the defined maximum energy of SEs.

Simulation Results and Discussion

Specimen Dependent and Analyser Geometry Dependent Effects

Figs. 6(a), (b) and (c) show the modified S-curves for three different collection criteria y_c of 0.5 mm, 1 mm and 2 mm, respectively for the case of a 10 V/mm extraction field and $(V_1, V_s, V_2) = (0, V_s, 0)$ V where V_s = 0, 1.5, 3, 5, 7.5 and 10 V. As was mentioned previously, a collection criteria y_c of 0.5 mm, means that only those SEs which are able to overcome the potential barrier and at the same time reach a level of 0.5 mm or greater above the specimen plane are considered as being collected. An increase in y_c can be viewed as a decrease in the width of the extraction grid with the distance between the specimen plane and the extraction grid remaining unchanged. It can be observed from these figures that as y_c increases, the modified S-curves for different specimen biases V_s no longer overlap each other. This deviation from the linearization relation is especially evident for the case of y_c = 2 mm in Fig. 6(c). One can estimate the amount of this deviation for the particular specimen bias V_s relative to the V_s = 0 V modified S-curve by calculating the difference in $(V_s - V_r)$, called $\delta(V_s - V_r)$. This deviation can be plotted in the form of

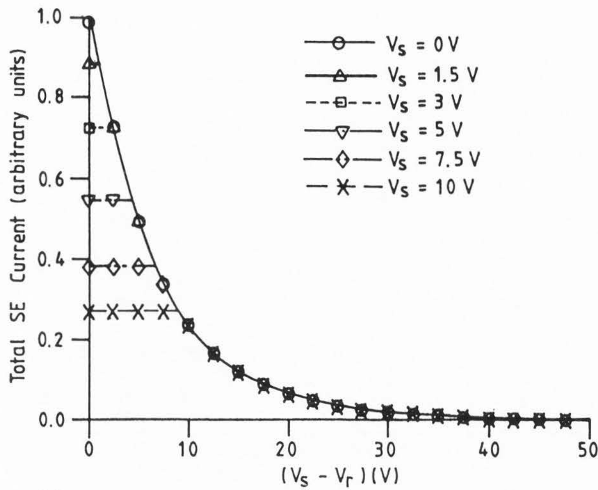

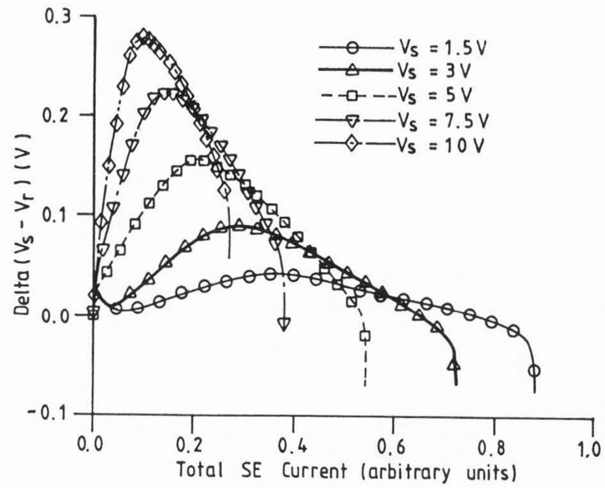

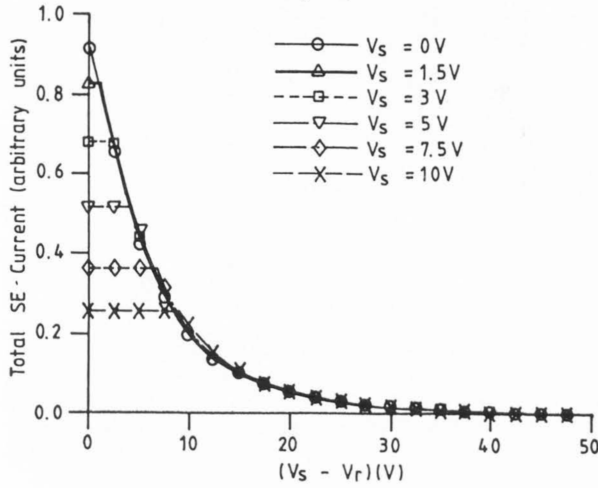

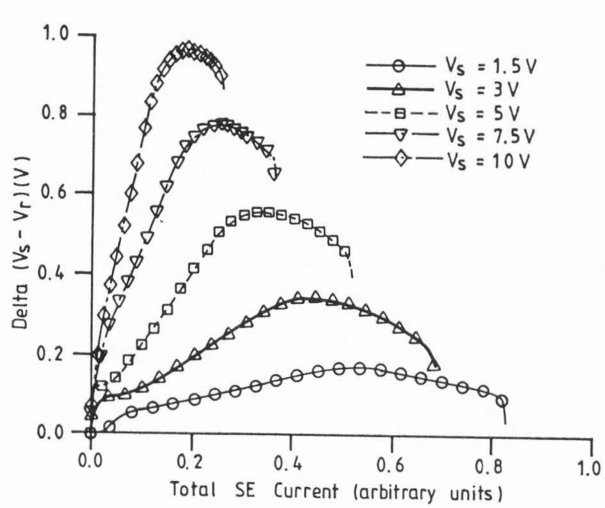

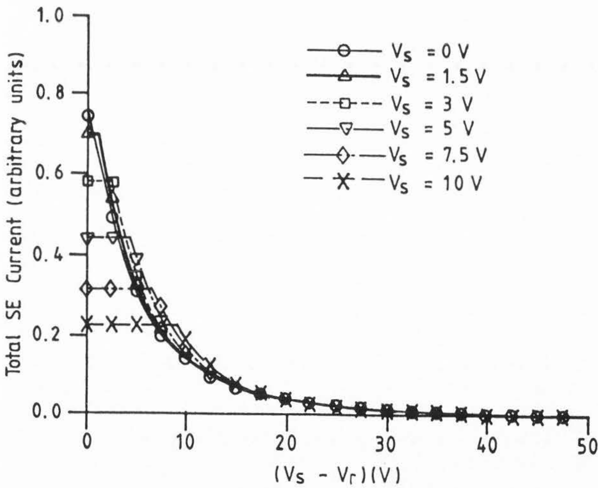

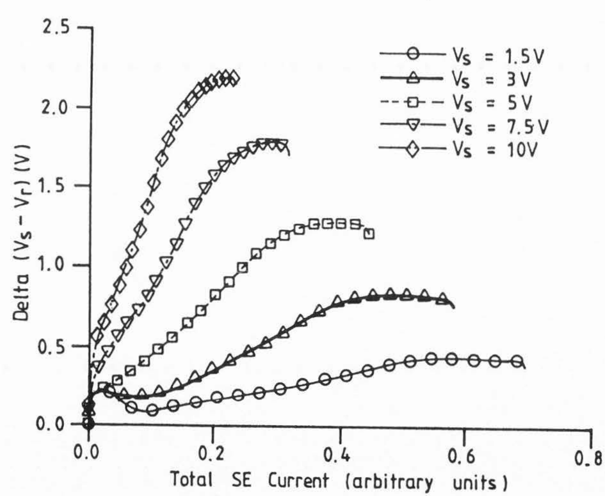

Fig. 6: Modified S-curves for $(V_1, V_s, V_2) = (0, V_s, 0)$ V for V_s = 0, 1.5, 3, 5, 7.5 and 10 V in a 10 V/mm extraction field and a collection criteria of (a) y_c = 0.5 mm, (b) y_c = 1 mm, and (c) y_c = 2 mm.

Fig. 7: Linearization error voltage curves for $(V_1, V_s, V_2) = (0, V_s, 0)$ V for V_s = 0, 1.5, 3, 5, 7.5 and 10 V in a 10 V/mm extraction field and a collection criteria of (a) y_c = 0.5 mm, (b) y_c = 1 mm, and (c) y_c = 2 mm.

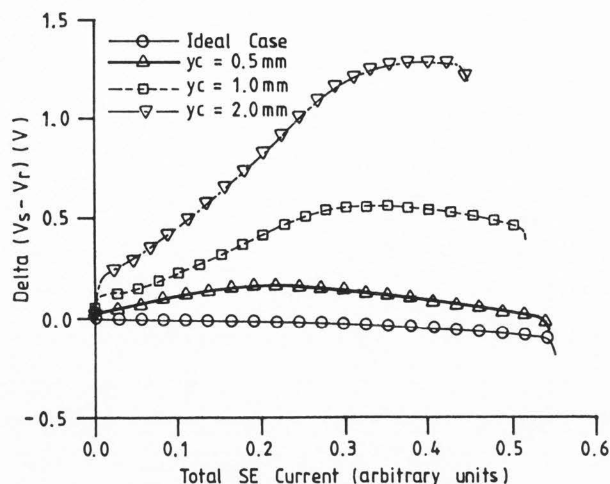

Fig. 8: Linearization error voltage curves for (V_1,V_s,V_2) = (0,5,0) V in a 10 V/mm extraction field for different collection criteria y_c equal to 0.5 mm, 1 mm and 2 mm. The ideal case corresponds to the situation where only the specimen dependent effect is present with the spatial dimension effect of the extraction grid being negligible.

linearization error voltage curves as shown in Figs. 7(a), (b) and (c) for y_c = 0.5 mm, 1 mm and 2 mm, respectively.

Fig. 8 compares the linearization error voltage curves for different y_c for the particular case of (V_1,V_s,V_2) = (0,5,0) V and a 10 V/mm extraction field. The ideal case corresponds to the situation where only the specimen dependent effect is present, with the spatial dimension effect of the extraction grid being negligible. In physical terms, the ideal case occurs when the width of the energy analyser is considered to be very large or infinite and all SEs which have sufficient energy to overcome the potential barrier set up by the local fields are considered to be collected. One can note from this figure that the linearization error voltage is quite small for the ideal case, the maximum being approximately 0.1 V in magnitude. However, this linearization error increases as the spatial dimension effect of the extraction grid becomes more pronounced and can be as large as 1.3 V for the case of y_c = 2 mm where the spatial dimension of the extraction grid is very small.

Influence of Extraction Field on Analyser Geometry Dependent Effect

The use of a large extraction field not only leads to a reduction in the potential barrier thereby causing a decrease in the local field effects, but also causes the SE trajectories to be directed towards the vertical axis of the energy analyser thereby causing a reduction in the analyser geometry dependent effect. Results of the simulation study have also revealed that y_c does not have a simple relationship with the effect of the extraction field. For example, if y_c is changed from 1mm to 2mm, the extraction field has to be increased from 10v/mm to 50v/mm in order to maintain linearization error voltage of the same magnitude. This is evident in Fig. 9. This relationship is also non-linear as can be seen from the different shapes of the curves in Fig. 9.

These results indicate that linearization errors can be divided into two components. The component attributable to specimen dependent effect (which in this case is the Type I local field effect) is relatively insignificant. However, the component due to analyser geometry effects becomes dominant when y_c is large. The physical reason for this effect is that not all

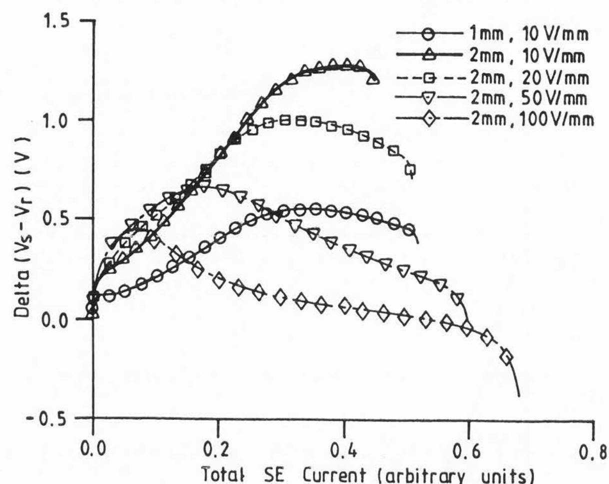

Fig. 9: Linearization error voltage curves for (V_1,V_s,V_2) = (0,5,0) V for different collection criteria y_c (given by the first parameter in mm in the legend) and different extraction fields (given by the second parameter in V/mm in the legend).

SEs which pass the potential barrier are collected, and the proportion of SEs going past the barrier which are collected varies with the specimen potential. This effect can be lessened to some extent by the application of large extraction fields. There are two implications arising from this result. Firstly, analysers having small widths introduce additional linearization errors to voltage measurements. Secondly, even for very wide analysers, linearization errors can be very large if the voltage measurement point on the specimen is near the edge of the analyser. This can happen if, for example, the specimen is very large when compared with the width of the analyser. Further work is being carried out to assess the importance of this effect in the case of large analysers.

Conclusions

This paper has presented a simulation model which can be used for studying and separating specimen dependent and analyser geometry dependent effects on the accuracy of quantitative voltage contrast. Simulation results show that the effect of analyser geometry on linearisation

error voltages can be substantial. However, these effects can be minimised by an appropriate choice of analyser dimensions.

References

[1] Chim WK, Low TS, Chan DSH, Phang JCH. (1988) Electron trajectory tracking algorithms for analysing voltage contrast signals in the scanning electron microscope. J. Phys. D: Appl. Phys. 21, 1-9.

[2] Chim WK, Phang JCH, Low TS, Chan DSH. (1987) An overview of quantitative voltage contrast measurements in the scanning electron microscope. Proceedings of the International Symposium on the Physical and Failure Analysis of Integrated Circuits Singapore 19-20 October 1987, 14-19, IEEE Singapore Section.

[3] De Jong JL, Reimer JD. (1986) Effects of local fields on electron beam voltage measurement accuracy. Scanning Electron Microsc. 1986; III:933-942.

[4] Feuerbaum HP. (1979) VLSI testing using the electron probe. Scanning Electron Microsc. 1979; I:285-296.

[5] Fleming JP, Ward EW. (1970) A technique for accurate measurement and display of applied potential distributions using the scanning electron microscope. Scanning Electron Microsc. 1970: 465-472.

[6] Fujioka H, Nakamae K, Ura J. (1981) Local field effects on voltage measurement using a retarding field analyser in the scanning electron microscope. Scanning Electron Microsc. 1981; I:323-332.

[7] Kollath R. (1966) Sekundarelektronen-Emission fester Korper bei Bestrahlung mit Electronen. Handbuch der Physik (Springer Berlin) 21, 232-303.

[8] Menzel E, Brunner M. (1983) Secondary electron analysers for voltage measurements. Scanning Electron Microsc. 1983; I:65-75.

[9] Nakamae K, Fujioka H, Ura J. (1981) Local field effects on voltage contrast in the scanning electron microscope. J. Phys. D: Appl. Phys., 14, 1939-1960.

[10] Nakamura H, Sato Y. (1983) An analysis of the local field effect on electron probe voltage measurements. Scanning Electron Microsc. 1983; III: 1187-1195.

[11] Nye P, Dinnis A. (1985) Extraction field and oxide charging in voltage contrast systems. Scanning 7, 117-124.

[12] Tee WJ, Gopinath A. (1976) A voltage measurement scheme for the SEM using a hemispherical retarding analyser. Scanning Electron Microsc. 1976; I:595-602.

[13] Ura J, Fujioka H, Nakamae K. (1984) Reduction of local field effect on voltage contrast. Scanning Electron Microsc. 1984; III:1075-1080.

Discussion with Reviewers

H. Fujioka: In the acceptance diagram (Fig. 5), the angle of the acceptance cone seems to be limited only by the width of the collection criteria plane. In the planar retarding field energy analyzer, however, it depends upon the ejection angle itself, because the retarding grid analyzes the longitudinal velocity component: the acceptance cone should have no flat boundary against the ejection angle. Could you please explain it?

Authors: In this study, we have tried to bring out the analyser geometry dependent effects. We have not taken into account the entry of the SEs into the retarding grid at non-vertical incidence angles. We believe that this will constitute a separate error component and is being studied separately. The inclusion of the off-incidence effect will modify the acceptance diagram, which otherwise will be flat as shown in Figure 5.

A.R. Dinnis: Consideration appears to be restricted to flat-grid analysers. Are the results applicable to analysers incorporating hemispherical grids and have you considered analysers in which the specimen is immersed in a magnetic field?

Authors: We have not considered the applicability of these results to hemispherical analysers.

A.R. Dinnis: In Figure 3, the equipotentials between 0.70 V and 0.8 V are rather strangely shaped. It seems likely that this is due to interpolation within meshes which are too coarse to give accurate detail at this level. I suggest that the figure should be modified; most simply by just removing these particular equipotentials. It would be better if a finer mesh were used, of course, and it would in any case be helpful if details of the mesh were given.

Authors: Extensive computation with fine mesh discretisation of the model have shown that the field structure described by Figure 3 represents a true and correct picture of the field distribution of the model. The shape of the potential distribution arises from the presence of the potential barrier.

The details of the mesh used in the computations are given as follows: The simulation model has dimensions 2mm by 2mm and is divided into 113 points along the horizontal axis and 58 points along the vertical axis. This gives rise

to 6554 nodes and 12768 triangular elements for the entire mesh. The smallest triangular elements are found around the specimen or 3-electrode structure, and these have sides of 0.5, 0.5 and 0.707 microns in length.

K.D. Herrmann: It is not clear how the "collection criterion Yc" is related to the real analyzer geometry (the width and the distance of the extraction grid). Is the width of the extraction grid fixed to 2 mm equal to the width of your model, and does the height of the collection plane Yc determine the solid angle of the SE-emission, which is not confined by the boundaries of your model and therefore can be detected?

K.D. Herrmann: If the above is true, why do you concentrate on an analyzer geometry with 2 mm width (width of the extraction grid) and extraction fields of 10 V/mm. Analyzers commonly in use exhibit widths of about 10 mm and extraction fields are in the order of 100 V/mm up to 1000 V/mm. If there do not exist specific applications or needs for such a narrow analyzer and such low extraction voltages, the influence of the analyzer geometry should be calculated for more realistic boundary conditions.

A.R. Dinnis: Computed results are given only for the exceptionally low extraction field of 10 V/mm. Are the results therefore of great significance for real analysers used on real circuits and do you have any practical confirmation of these results?

Authors: The analyser dimension of 2mm is the width of the extraction grid in the model. The choice of 2mm enables a more accurate calculation of the electric field as a much finer mesh can then be used. Having fixed this value, the variation of y_c is used to study the severity of geometry dependent effects. The relationship between y_c and the width of the extraction grid is non-linear and can be approximated by a square law relationship for a particular constant extraction voltage and SE energy.

From our studies of error voltages with 10V/mm and 100V/mm extraction fields, we expect that a higher extraction field will reduce the geometry dependent effects. However, these geometry dependent effect errors will still be present especially for circuits near the edge of detectors. We do not at present have any practical confirmation of these results. The choice of 2mm is essentially for the accurate modelling of the field structure. The use of low extraction voltages is motivated by the recent trends towards low voltage operation in SEMs (see for example Nye and Dinnis, ref [11] in our paper; and Editorial in Scanning Vol 10, 1, (1988).)

H. Fujioka: By using the simulation model, have you estimated type II local field effects?

Authors: We have used the simulation model for the estimation of Type II local field effects, but not in relation to the analyser geometry dependent effects. This model can be applied to study Type II local field effects in detail.

A.R. Dinnis: In the paper you state that very low extraction fields are necessary to avoid interference with low-voltage primary beams. This is not always true, as evidenced by various commercial e-beam testers which produce acceptable spatial resolution despite the use of very much higher extraction fields than are examined in this paper. Please comment.

Authors: There are other advantages of low extraction field operation besides the avoidance of interference with the low voltage primary beam. For example, as stated in Nye and Dinnis [11], high extraction fields have undesirable effects on oxide charging and this in turn can have great influence on quantitative measurements due to the presence of strong surface fields. It has also been observed that high extraction voltages lead to a stretching of the S-curve with consequent loss of voltage resolution, and very high voltages can cause severe distortion of the curve.